Molecular Biology of the Cell
Vol. 21, 1188–1199, April 1, 2010

PICH and Cotargeted Plk1 Coordinately Maintain Prometaphase Chromosome Arm Architecture

Yasuhiro Kurasawa*† and Li-yuan Yu-Lee*‡§‖

*Department of Medicine, Section of Immunology Allergy and Rheumatology, ‡Department of Molecular and Cellular Biology, §Department of Immunology, and ‖Cell and Molecular Biology Program, Baylor College of Medicine, Houston, TX 77030

Submitted November 13, 2009; Revised January 20, 2010; Accepted January 25, 2010
Monitoring Editor: Yixian Zheng

To maintain genomic stability, chromosome architecture needs to be tightly regulated as chromosomes undergo condensation during prophase and separation during anaphase, but the mechanisms remain poorly understood. Here, we show that the Plk1-binding protein PICH and Plk1 kinase coordinately maintain chromosome architecture during prometaphase. PICH knockdown results in a loss of Plk1 from the chromosome arm and an increase in highly disorganized "wavy" chromosomes that exhibit an "open" or "X-shaped" configuration, consistent with a loss of chromosome arm cohesion. Such chromosome disorganization occurs with essentially no change in the localization of condensin or cohesin on chromosomes. Interestingly, the chromosome disorganization could be prevented by treatment with a topoisomerase II inhibitor ICRF-193, suggesting that the PICH–Plk1 complex normally maintains chromosome architecture in a manner that involves topoisomerase II activity. PICH knockdown does not affect initial chromosome compaction at prophase but causes anaphase DNA bridge formation and failed abscission. Our studies suggest that the PICH–Plk1 complex plays a critical role in maintaining prometaphase chromosome architecture.

INTRODUCTION

Faithful transmission of the genome to daughter cells requires the coordination of major chromosomal events during mitosis, including chromosome condensation and sister chromatid resolution, cohesion, and separation. Previous studies suggest that two chromosomal proteins topoisomerase II (Topo II) (Newport and Spann, 1987; Uemura *et al*., 1987; Wood and Earnshaw, 1990; Adachi *et al*., 1991; Gorbsky, 1994) and condensin (Hirano and Mitchison, 1994; Saka *et al*., 1994) are important for chromosome condensation. Recent knockdown studies showed that Topo II and condensin contribute to the proper timing of sister chromosome resolution, stabilization of already condensed chromosomes, and proper chromosome segregation (Hirano, 2005; Belmont, 2006; Xu and Manley, 2007).

Chromosome cohesion is mediated by a multiprotein cohesin complex (Guacci *et al*., 1997; Michaelis *et al*., 1997; Losada *et al*., 1998) that is loaded onto chromosomes during S phase and removed in a stepwise manner from chromosomes by different mechanisms to allow sister chromosomes to separate during mitosis. These include bulk cohesin removal from chromosome arms after Plk1- and Aurora B-mediated phosphorylation (Losada *et al*., 2002; Sumara *et al*., 2002; Gimenez-Abian *et al*., 2004; Hauf *et al*., 2005) of cohesin subunits and by association with a cohesin-binding protein Wapl during prophase (Gandhi *et al*., 2006; Kueng *et al*., 2006), and cleavage of the cohesin subunit Scc1 by separase (Uhlmann *et al*., 2000) at the centromere during anaphase. However, recent cohesin knockdown (Vagnarelli *et al*., 2004; Deehan Kenney and Heald, 2006; Toyoda and Yanagida, 2006; Diaz-Martinez *et al*., 2007) and other studies (Sullivan *et al*., 2004; Diaz-Martinez *et al*., 2006; Baumann *et al*., 2007; D'Ambrosio *et al*., 2008; Wang *et al*., 2008) suggest that in addition to the cohesin complex physically entrapping sister chromatids, chromosome cohesion also involves interchromatid catenations that intertwine sister chromatids (Diaz-Martinez *et al*., 2008). To what extent DNA catenation contributes to sister chromatid cohesion remains unclear. The resolution of such DNA catenations is mediated by the DNA decatenating enzyme Topo II (Clarke and Lane, 2009; Nitiss, 2009). However, how Topo II activity for chromosome separation is regulated remains unknown.

A helicase-like protein PICH is found as a Plk1-binding protein (Baumann *et al*., 2007). PICH is localized at the centromere and can be detected on "threads" that are thought to contain unresolved catenated DNA between separating centromeres during anaphase (Baumann *et al*., 2007; Wang *et al*., 2008). PICH was initially suggested to act as a tension-sensing spindle checkpoint regulator at the kinetochore (Baumann *et al*., 2007), but this function was questioned in a recent work done by the same group (Hubner *et al*., 2010). PICH also has been suggested to contribute to chromosome compaction through its ATPase domain (Leng *et al*., 2008). Here, we show that PICH knockdown resulted in a loss of chromosome arm cohesion and chromosome organization. Furthermore, this chromosome disorganization phenotype could be prevented by treatment with a Topo II inhibitor. Thus, our studies suggest that the PICH–Plk1 complex functions to maintain chromosome architecture.

This article was published online ahead of print in *MBoC in Press* (http://www.molbiolcell.org/cgi/doi/10.1091/mbc.E09–11–0950) on February 3, 2010.

† Present address: Department of Genetics, University of Texas M.D. Anderson Cancer Center, Houston TX 77030.

Address correspondence to: Li-yuan Yu-Lee (yulee@bcm.edu).

MATERIALS AND METHODS

Antibodies

Antibodies were used for immunofluorescence (IF) and immunoblotting (IB) at the following concentrations. Mouse anti-Plk1 (F-8 [Santa Cruz Biotechnology, Santa Cruz, CA], 1:1000–1:1500 for IF, 1:1500 for IB; and PL2+PL6 [Zymed Laboratories, South San Francisco, CA], 1:500 for IF), rabbit anti-Plk1 (H-152 [Santa Cruz Biotechnology], 1:1000 for IF; and ab14209 [Abcam, Cambridge, MA], 1:400–500 for IF), mouse anti-PICH (anti-FLJ20105 3F12-2B10 [Abnova, Taipei, Taiwan], 1:1000 for IF, 1:2000 for IB), rabbit MP-PAb1 (mitotic phosphoprotein polyclonal antibody 1; see Supplemental Figure 1; 1:400–1500 for IF, 1:2000–4000 for IB), rabbit anti-SMC2 (A300-058A [Bethyl Laboratories, Montgomery, TX], 1:1000–1500 for IF, 1:1000 for IB), rabbit anti-topoisomerase IIa (2011-1 [TopoGEN, Port Orange, FL], 1:1000 for IF), rabbit anti-Scc1 (from Dr. Jun Qin [Baylor College of Medicine, Houston, TX], 1:250 for IF), rabbit anti-Mad2 (BL1462 [Bethyl Laboratories], 1:400–1000 for IF), rabbit anti-Cdc20 (Santa Cruz Biotechnology, 1:1000 for IB), mouse anti-β-tubulin (tub2.1 [Sigma-Aldrich, St. Louis, MO], 1:2000 for IB), and rabbit anti-phospho-histone H3 (Ser10) (Millipore, Billerica, MA, 1:1000 for IB). Secondary antibodies conjugated to Texas Red, Alexa Fluor 488, and Alexa Fluor 594 (Invitrogen, Carlsbad, CA, 1:1000) were used for immunofluorescence and those conjugated to horseradish peroxidase (Vector Laboratories, Burlingame, CA, 1:10000–15000) were used for immunoblot detection.

Cell Lysates, Immunoblotting, Phosphatase Treatment, and Coimmunoprecipitations

Cells were harvested with a scraper (or by shake-off in case of nocodazole-arrested lysate) and lysed in the lysis buffer (0.5% Triton X-100, 150 mM NaCl, 5 mM EGTA, 1.5 mM EDTA, 5% glycerol, and 50 mM Tris-HCl pH 8.0) supplemented with 1 mM phenylmethylsulfonyl fluoride; 5 mM Na_3VO_4; 5 mM NaF; 200 nM microcystin-LR; and mammalian protease-, serine-threonine phosphatase-, and tyrosine phosphatase-inhibitor cocktails (all from Sigma-Aldrich). For immunoblotting, samples were prepared by adding NuPAGE LDS sample buffer (Invitrogen) with 2% β-mercaptoethanol, resolved by Novex-NuPAGE-gel (Invitrogen) and transferred to nitrocellulose membrane (Bio-Rad Laboratories, Hercules, CA). Membrane was blocked with 5% nonfat milk in Tris-buffered saline (TBS; 137 mM NaCl and 20 mM Tris-HCl, pH 7.6) at room temperature for 1 h, incubated with primary (4°C; >3 h) and secondary (1–2 h at room temperature) antibodies in 0.1% Tween 20 in TBS (TBS-T) containing 5% bovine serum albumin (BSA) and processed for chemiluminescence SuperSignal West Pico (Pierce Chemical, Rockford, IL). Between each step, membrane was washed in TBS-T three times for a total of >30 min. For coimmunoprecipitations, 1 mg of lysates (in 250 μl) was precleared by incubation for 1 h with protein G-Sepharose beads (GE Healthcare, Piscataway, NJ) and then incubated with both 1.5 μl of each antibody and protein G-Sepharose at 4°C overnight. The beads were washed four times

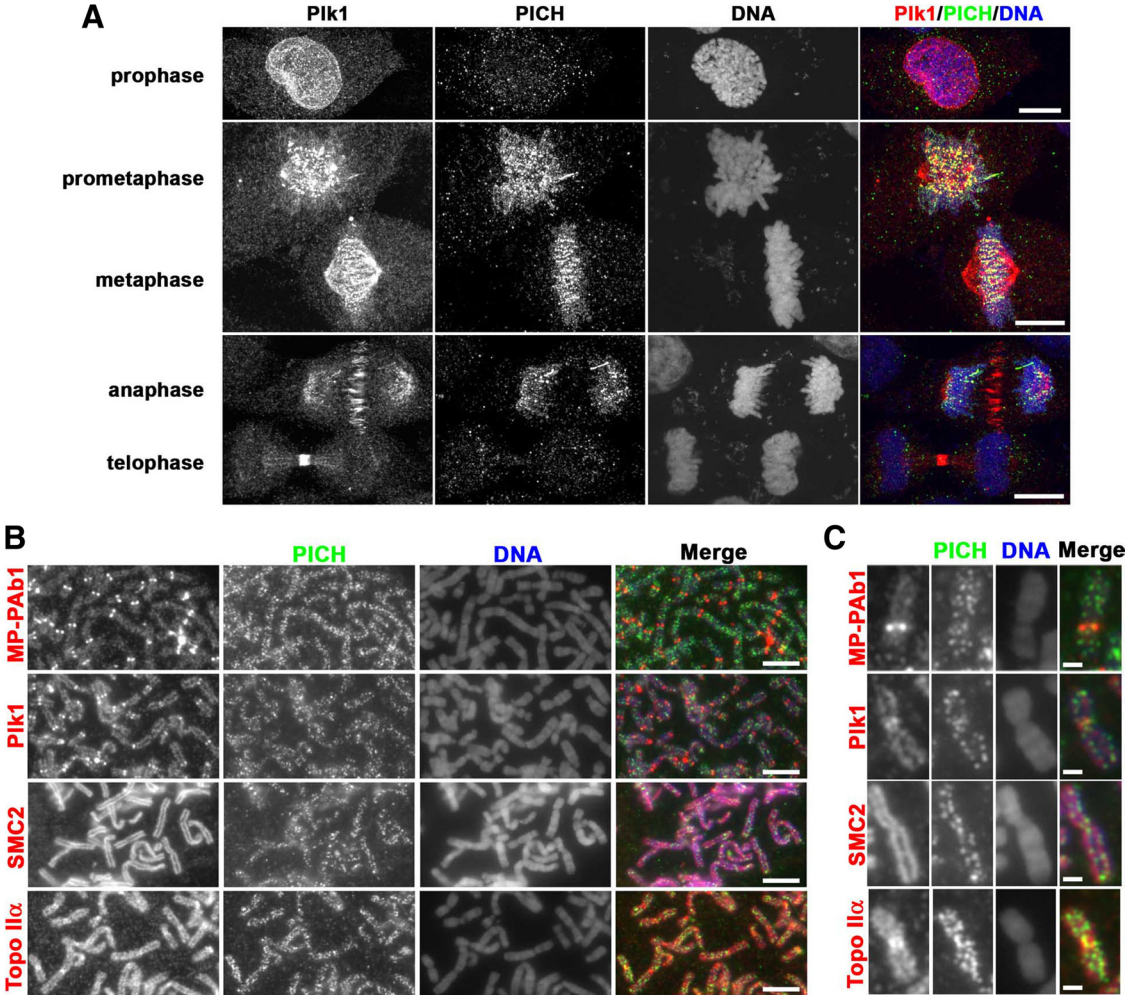

Figure 1. PICH and Plk1 colocalize on mitotic chromosome arms. (A) HeLa cells undergoing unperturbed mitosis were stained with anti-PICH (green) and anti-Plk1 (red) antibodies and counterstained with DAPI (blue) and then analyzed by confocal microscopy. Images with single antibody staining are shown in black and white for better contrast. Bars, 10 μm. Note, PICH-positive "threads" in an anaphase cell. (B) HeLa cells were treated with 2 mM thymidine for 14.5 h, released for 6.5 h, and incubated with 25 ng/ml nocodazole for 1.5 h. Chromosome spread preparations were made as described in *Materials and Methods*, and chromosomes were stained for PICH together with Plk1, condensin SMC2, or Topo IIα as indicated. MP-PAb1 that was used to isolate PICH (see Supplemental Data) also stained the kinetochore intensely. Bars, 5 μm. (C) Magnified images of selected chromosomes in B. Note that the kinetochore localization of PICH is more readily detected in fixed cells (A) than in the chromosome spread preparations (B and C). Bars, 1 μm.

with lysis buffer, and the bound proteins were eluted in the sample buffer and then analyzed by immunoblotting. For partial purification of the 150-kDa protein, mitotic lysate (85 mg) was precleared for 1- to 2-h incubation with protein G-Sepharose preincubated with normal goat serum once and then with protein G-Sepharose twice. The precleared lysate was used for the initial immunoprecipitation with 85 μl of Plk1 (F-8) antibody. Proteins bound to Plk1–immunoprecipitate beads were quickly eluted with 200 μl of 0.1 M glycine-HCl, pH 3.0, three times. Combined eluents were immediately neutralized by adding 90 μl of 0.2 M Tris-HCl, pH 8.8, and 690 μl of lysis buffer and then used for the second immunoprecipitation with MP-PAb1 antibody. Purification steps of the 150-kDa protein were checked by SDS-polyacrylamide gel electrophoresis followed by either silver staining or immunoblotting with MP-PAb1 antibody. For phosphatase treatment, membranes containing transferred proteins were washed with a phosphatase buffer (1 mM $MgCl_2$, 0.1 mM $ZnCl_2$, 1 mM spermidine, and 50 mM Tris-HC1 pH 9.3), incubated with or without 10 U/ml calf intestinal alkaline phosphatase (Promega, Madison, WI) in the buffer at 37°C for 5 h and subjected to immunoblot analysis.

Cell Culture and Synchronization

HeLa cells were cultured in DMEM supplemented with 10% fetal bovine serum (FBS). HeLa cells stably expressing green fluorescent protein (GFP)-tagged histone H2B (BD Biosciences Pharmingen, San Diego, CA) were generated by cotransfection of the H2B-GFP vector with a blasticidin-resistant construct at a 10:1 ratio, followed by selection with blasticidin. To enrich for mitotic cells, HeLa cells were cultured with 2 mM thymidine (Sigma-Aldrich) for ~12–16 h and then either released into fresh medium for 6.5–7.5 h, or released for 5.5–7 h in fresh medium followed by an incubation with 25–100 ng/ml nocodazole (Sigma-Aldrich) plus 20 μM MG132 (Calbiochem, San Diego, CA) (noc/MG132) for 2–5 h, depending on the experiment. In some experiments, two cycles of thymidine block and release was used. To obtain highly synchronized mitotic progression, cells were synchronized with a thymidine block and then enriched at the G2/M phase boundary by an incubation with 9 μM RO-3306 (Vassilev *et al.*, 2006) (Calbiochem) for 10–13 h. Next, they were released either into regular medium for live-cell imaging analysis or medium containing noc/MG132 for chromosome spread preparations. For all synchronization protocols, cells were washed with prewarmed (37°C) medium in between steps for the best results. For Topo II inhibition, 20 μM ICRF-193 (BIOMOL Research Laboratories, Plymouth Meeting, PA) or dimethyl sulfoxide (DMSO) vehicle was added to mitotic cells.

RNA Interference and Transient DNA Transfection

HeLa cells were transfected with 100 nM small interfering RNA (siRNA) duplexes for control siCONTROL#2, PICH (Leng *et al.*, 2008) (5′-GTTATGCTCTTGACTTTAA-3′), Plk1 (Ahonen *et al.*, 2005) (5′-GATCACCCTCCTTAAATAT-3′), and Mad2 (Stegmeier *et al.*, 2007) (5′-CTATTGAATCAGTTTCCAA-3′) (all from Dharmacon RNA Technologies, Lafayette, CO) using oligofectamine (Invitrogen) according to the manufacturer's protocol. For PICH knockdown, cells were transfected with PICH siRNA oligonucleotides (oligos), synchronized using either thymidine or RO-3306 treatment, and analyzed 2 d after transfection. For Plk1 knockdown, cells were cultured for 26 h after Plk1 siRNA oligo transfection and then treated with 25 ng/ml nocodazole for 4 h. For Mad2 knockdown, cells were analyzed 2 d after Mad2 siRNA oligo transfection. Plasmid transfection was performed using Lipo-

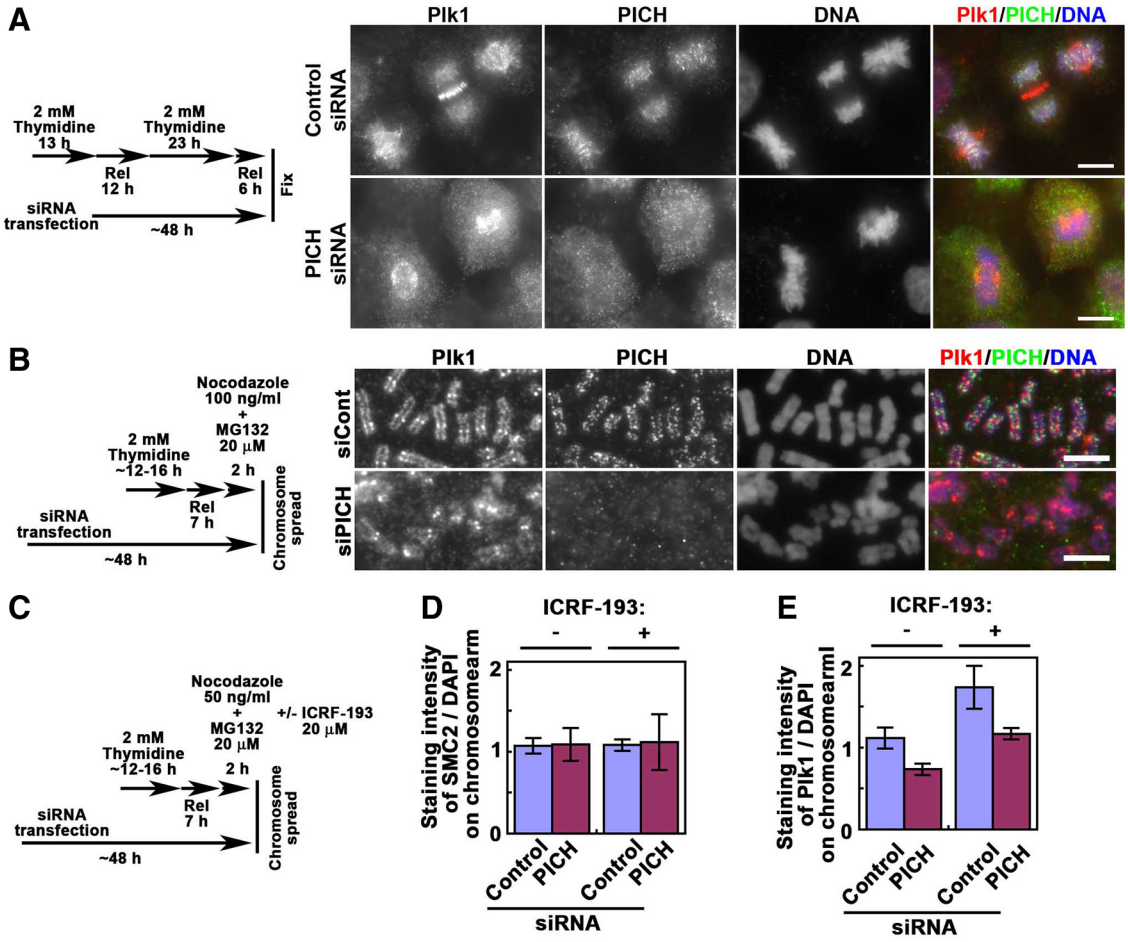

Figure 2. PICH regulates Plk1 targeting to the chromosome arm. (A and B) HeLa cells were transfected with control or PICH-specific siRNA oligo using protocols indicated on the left. Fixed cell (A) or chromosome spread (B) preparations were stained with anti-PICH (green) and anti-Plk1 (red) antibodies and counterstained with DAPI (blue). Bars, 10 μm (A) and 5 μm (B). (C–E) Chromosome spreads were prepared from siRNA-transfected HeLa cells that were treated with or without 20 μM ICRF-193, a Topo II inhibitor, for 2 h and then costained for condensin SMC2 and Plk1 and counterstained with DAPI (C). The fluorescence intensities of SMC2 (D) or Plk1 (E) staining on chromosomes were normalized against that of DAPI on the same chromosome arm region (see *Materials and Methods*). Values ± SEM were obtained from >80 chromosomes (5 chromosomes/spread) evaluated in three independent experiments (n = 3).

fectamine 2000 (Invitrogen) according to the manufacturer's protocol specific for HeLa cells. Cells transfected with wild type GFP-PICH (GFP-PICH-WT) or GFP-PICH-TA containing a T1063A mutation (Leng *et al.*, 2008) for 24 h were treated with 100 ng/ml nocodazole for 2 h and harvested for chromosome spread analysis (see below).

Indirect Immunofluorescence

HeLa cells were cultured on coverslips, rinsed twice with prewarmed PHEM (60 mM piperazine-*N*,*N*′-bis(2-ethanesulfonic acid) [PIPES], 25 mM HEPES, 10 mM EGTA, and 2 mM $MgCl_2$, pH 6.9 with KOH), permeabilized with 0.5% Triton X-100 in PHEM at 4°C for 1 min, and fixed with 4% paraformaldehyde in PHEM at 4°C for 20 min. For Scc1 staining, permeabilized cells were fixed in 1% paraformaldehyde in PHEM at 4°C for 5 min. The fixed cells were incubated at 4°C for 1 h with an antibody blocking solution (0.1 M PIPES, 1 mM $MgSO_4$, 1 mM EGTA, 1.83% L-lysine, 1% BSA, and 0.1% NaN_3, pH 7.2 with KOH, presaturated with nonfat milk at 4°C) and then incubated overnight with primary antibody followed by secondary antibody plus 100 ng/ml 4,6-diamidino-2-phenylindole (DAPI) for 3 h. Samples were mounted in ProLong Gold antifade reagent with DAPI (Invitrogen). Between each step, cells were quickly washed twice with ice-cold phosphate-buffered saline.

Chromosome Spread

Mitotic HeLa cells were synchronized and treated with noc/MG132 as described above and collected by gentle pipetting. Cells were transferred to another tube, briefly centrifuged, and the residual medium around the cell pellet was completely removed. For swelling, the cell pellet was suspended in 1 ml of prewarmed (37°C) hypotonic solution (55 mM KCl and 50 ng/ml nocodazole) and incubated at room temperature for 5 min followed by 4°C for 1.5 min. The swollen cell suspension (1.4×10^4 cells/0.2 ml) was transferred into a Cytospin Cytofunnel (Thermo Fisher Scientific, Waltham, MA) that was prefilled with a glycerol solution (3% glycerol, 55 mM KCl, and 3 mM Tris-HCl, pH 6.8, [4°C; 0.4 ml]). A coverslip was assembled between the Cytofunnel and a glass slide. Cells were spun onto the coverslip at 1500 rpm for 2 min. The coverslip was quickly removed to avoid drying and immediately processed for indirect immunofluorescence as described above.

Microscopy and Fluorescence Intensity Measurements

Images were acquired using a D-Eclipse C1 confocal laser scanning microscope or a TE2000 widefield microscope system (both from Nikon, Tokyo, Japan). Confocal images were acquired as z-stacks with a step size of 0.2 μm by using a 60× oil/1.40 numerical aperture objective, and maximal intensity projections of all optical sections are shown. For quantification of fluorescence intensities, a chromosome region was marked as a region of interest (ROI). The average intensity of signals in the ROI for both the Plk1 channel and the SMC2 channel were obtained, and background signals obtained from the vicinity outside of the chromosomes were subtracted from the measurements. The signals were then normalized against that of DAPI from the ROI to generate the actual intensities on the chromosome arm, by using NIS-Elements (Nikon) software. Five chromosomes were measured from each single spread, and >80 chromosomes were measured.

Live-Cell Time-Lapse Imaging

Cells cultured in a glass-bottom dish (VWR, West Chester, PA) were synchronized using the RO-3306 treatment for G2/M phase enrichment. After quickly rinsing twice with prewarmed medium and replacing with fresh medium, the culture dish was placed into the live-imaging chamber in a Nikon BioStation IM to let settle for 5 min. Multiple image capture points and the focal plane (11 μm higher than the focusing plane at the center of the dish) were selected, and image capture was initiated 10 min after the release from G2/M arrest. Images were acquired every 2 min and compiled using NIS-Elements software.

Detecting Connected Cells by Trypsin Treatment

Cells cultured in a 12-well plate were treated with 10–15 μl of 0.05% trypsin-EDTA (Invitrogen), incubated at 37°C for 4 min, gently suspended in 0.5 ml of culture medium, and centrifuged. After removing 0.4 ml of the supernatant, cells were resuspended in the remaining 0.1 ml of medium, mixed with 0.5 ml of a hypotonic solution (40% culture medium containing FBS and 60% water; 37°C), and incubated for 5 min at room temperature. To fix the cells, 0.2 ml of 16% paraformaldehyde (Electron Microscopy Science, Hatfield, PA) was added to the cell suspension and incubated at room temperature for 20 min. After a brief centrifugation, cells were resuspended in 50 μl of the remaining fixation solution, spread over a coverslip, and excess liquid around the cells were gently removed by aspiration. Cells were dried onto the coverslip for 3 min, treated with 0.25% Triton X-100 in PHEM for 10 min, and mounted in 100% glycerol.

Statistical Analysis

Data were confirmed in multiple independent experiments. Data quantification was performed by using the Student's *t* test and expressed as mean ± SD or mean ± SEM. p values of <0.05 were considered statistically significant.

RESULTS

PICH Targets a Subpopulation of Plk1 to Chromosome Arms at Prometaphase

We originally isolated a 150-kDa Plk1-binding protein as the recently identified PICH ATPase (Baumann *et al.*, 2007), from biochemical studies of a mitotic phosphoepitope antibody MP-PAb1 (see Supplemental Material and Supplemental Figure 1). In addition to localizing at the centromere and on anaphase thread structures (Baumann *et al.*, 2007), PICH is also found on chromosome arms in GFP-PICH overexpression studies (Leng *et al.*, 2008). Here, we examined endogenous PICH localization over mitosis by confocal microscopy analysis. PICH is not detected in the nucleus before nuclear envelope breakdown in prophase, but it is localized at the kinetochore and chromosome arm during prometaphase and metaphase, and it remains on DNA in anaphase, often enriched on thread-like structures (Figure 1A). Using chromosome spreads for higher resolution, we found that PICH exhibits a punctate staining pattern along the chromosome arm (Figure 1, B and C). This punctate pattern is different from the more uniform staining pattern observed for Plk1, Topo IIα and a condensin component SMC2 on the chromosome arm (Figure 1, B and C). Plk1 is clearly seen on the axis of the chromosome arm, using four different anti-Plk1 antibodies (Supplemental Figures 1D and 2). PICH staining partially overlapped with Plk1 staining (Figure 1, B and C). The specificities of PICH (Figure 2, A and B, and

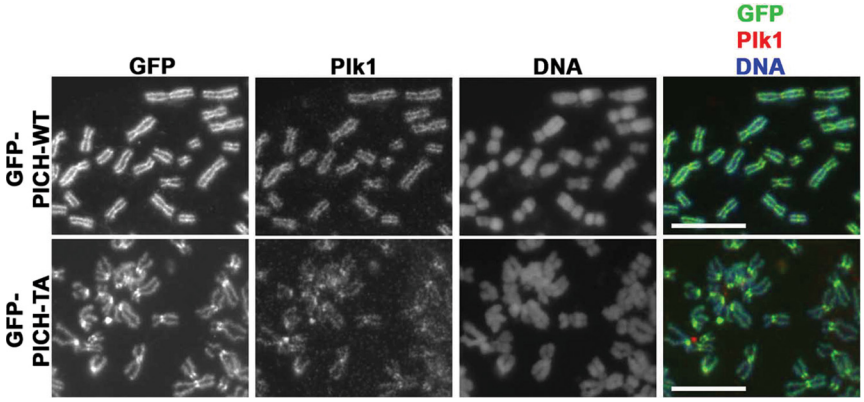

Figure 3. Overexpression of GFP-PICH-TA mutant causes mistargeting of Plk1 from the chromosome arm and a loss of chromosome arm cohesion. HeLa cells were transfected with a GFP-PICH wild-type construct (GFP-PICH-WT) or a PICH mutant construct (GFP-PICH-TA), which contains a mutation (T1063A) in a Cdk1 phosphorylation site, that can no longer bind to Plk1 and target Plk1 to the chromosome arm (Leng *et al.*, 2008). Chromosome spreads were prepared and GFP-positive spreads (green) were stained for Plk1 (red) and counterstained with DAPI (blue). Bars, 10 μm.

Supplemental Figure 1E) and Plk1 (Supplemental Figures 1E and 2) staining on chromosome arms were confirmed by siRNA-based knockdowns. Interestingly, unlike in fixed cells (Figure 1A), PICH was not readily detectable at the kinetochore in chromosome spreads (Figure 1, B and C), as such preparations required a nocodazole treatment that destroys microtubules, which suggests that kinetochore tension might promote PICH accumulation at the centromere (Baumann *et al.*, 2007). Note that PICH staining on chromosomes increased in the Plk1 knockdown cells (Supplemental Figure 2) as described previously (Baumann *et al.*, 2007).

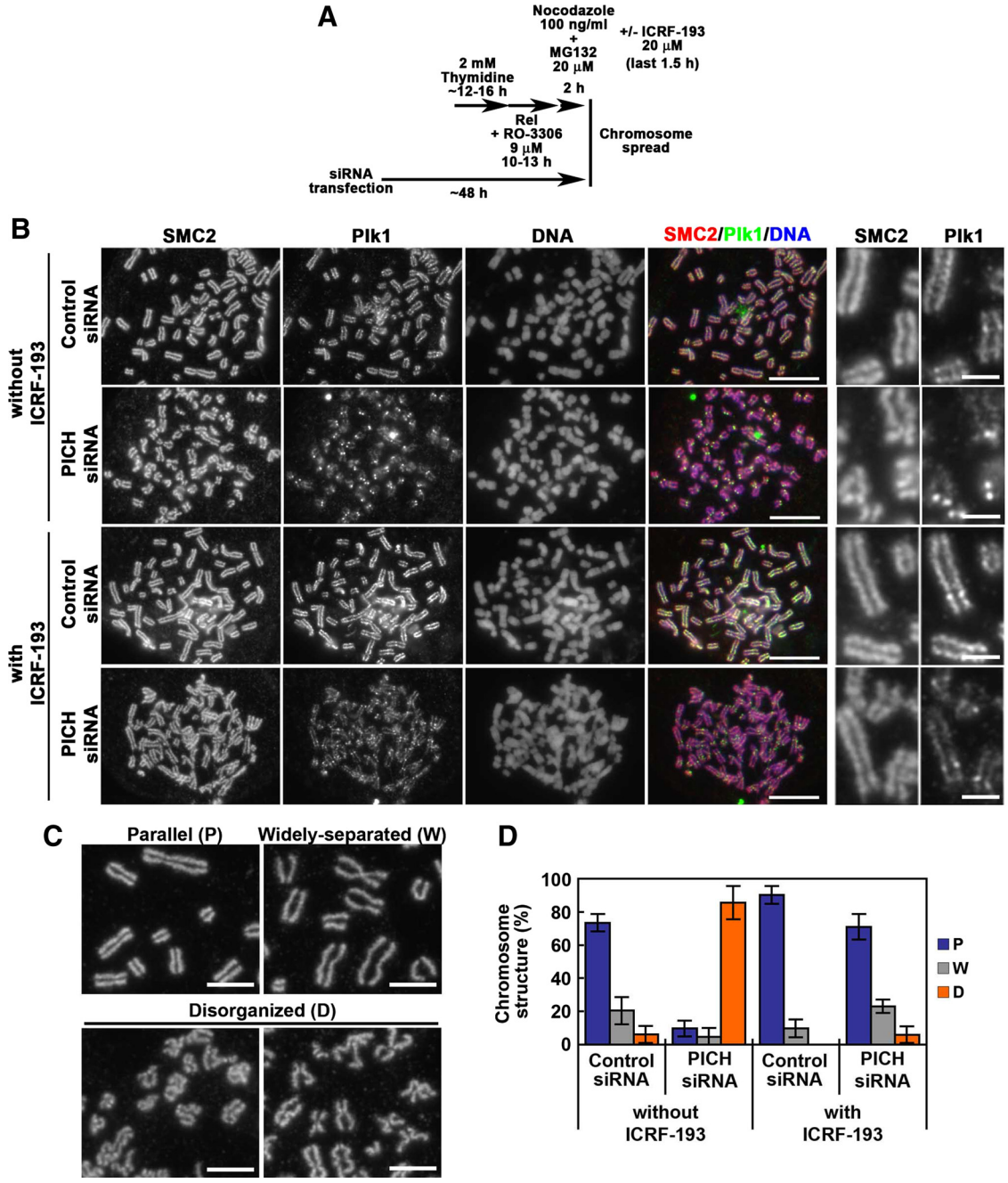

Figure 4. PICH depletion results in disorganized chromosomes and a loss of chromosome arm cohesion, which could be prevented by treatment with a Topo II inhibitor ICRF-193. (A) HeLa cells were treated with siRNA for control or PICH for ~48 h. Cells were treated with 2 mM thymidine for ~12–16 h, released into media containing 9 μM Cdk1 inhibitor RO-3306 for 10–13 h, and incubated with nocodazole plus MG132 for 30 min. Then, ICRF-193 or DMSO was added and further incubated for 1.5 h. (B) Chromosome spreads of cells treated as in A were prepared and stained with anti-SMC2 (red) and anti-Plk1 (green) antibodies and counterstained with DAPI (blue). Magnified images of chromosomes in the left panels (bars, 10 μm) are shown in the right panels (bars, 2 μm). (C) Chromosomes prepared as in A were stained with anti-SMC2. Chromosome morphologies were classified into three categories: parallel (P) for normal chromosome organization and chromosome arm cohesion, widely separated (W) for normal chromosome organization but widely separated chromosome arms, and disorganized (D) for loss of both chromosome organization and arm cohesion. Bars, 5 μm. (D) Quantification of chromosome structures classified as in C in cells treated as in B. The data represent the mean percentage ± SD obtained from at least 60 chromosome spreads in three independent experiments (n = 3).

We found that knockdown of PICH resulted in a reduction of Plk1 on chromosome arms, whereas Plk1 localization at the centrosome, spindle and kinetochore remained unchanged (Figure 2A). Quantification of Plk1 fluorescence intensity using chromosome spreads (Figure 2C) showed that PICH knockdown resulted in a 33.8% reduction of Plk1 on chromosome arms (Figure 2, B and E; $p = 2.52 \times 10^{-2}$). For comparison, the fluorescence intensity of condensin SMC2 that was costained with Plk1 on the same chromosome region remained essentially unchanged (Figure 2D). The fact that Plk1 was clearly detected at the kinetochore even as it was reduced on the chromosome arm (Figure 2, B and E) strongly suggests that Plk1 targeting to the kinetochore versus chromosome arms may be regulated differently. However, we noticed that Plk1 accumulates on DNA during prophase, at a time when PICH is not detected in the nucleus (Figure 1A). This observation suggests that Plk1 on chromosome arms may consist of two subpopulations: one population that is recruited to chromosomes during prophase and another that is targeted by PICH in prometaphase. That PICH targets Plk1 to the chromosome arm was further supported by overexpression studies in which GFP-PICH was found to colocalize with Plk1 on the chromosome arms. In contrast, a mutant GFP-PICH containing a T1063A mutation, which no longer binds to Plk1 and seemed to be more concentrated at centromeres, was unable to target Plk1 to the chromosome arms (Figure 3) (Leng *et al.*, 2008). Together, the PICH knockdown as well as overexpression studies clearly show that PICH is involved in targeting Plk1 to the chromosome arms.

PICH Depletion Results in a Disorganized Chromosome Structure and a Loss of Chromosome Arm Cohesion

Dissociation of cohesin from chromosome arms is partly regulated by Plk1 (Losada *et al.*, 2002; Sumara *et al.*, 2002; Gimenez-Abian *et al.*, 2004; Hauf *et al.*, 2005). Because PICH depletion resulted in a significant reduction of Plk1 from chromosome arms, we next investigated whether chromosome cohesion might be perturbed. PICH knockdown cells were synchronized with 2 mM thymidine; released for 10–13 h into media containing 9 μM RO-3306, a Cdk1 inhibitor that arrests cells at the G2/M transition (Vassilev *et al.*, 2006); and incubated with 100 ng/ml nocodazole and 20 μM MG132 for 2 h. Then, chromosome spreads were prepared (Figure 4A). Unexpectedly, cohesion between sister chromatids was not enhanced but instead was lost in PICH knockdown cells (Figure 4B, without ICRF-193). Careful examination revealed that PICH depletion led to a highly disorganized chromosome structure (Figure 4C, disorganized), in which the chromosome arms seemed to be more condensed and "wavy," and sister chromatid arms showed an "open" or "X-shaped" configuration that is consistent with a loss of arm cohesion. We quantified the chromosome morphologies into three categories, based on the degree of chromosome organization and sister chromatid cohesion (Figure 4, C and D): parallel (P) for normal chromosome organization and chromosome arm cohesion, widely separated (W) for normal organization but loss of arm cohesion, and disorganized (D) for loss of both chromosome organization and arm cohesion. Although the majority of chromosomes in control cells showed normal parallel chromosome morphology (73.4%; Figure 4D, without ICRF-193), in contrast the majority of chromosomes in PICH-deficient cells showed a disorganized, wavy chromosome arm structure (85.6%; Figure 4D, without ICRF-193; $p = 2.62 \times 10^{-4}$). Because control cells exhibited a normal chromosome structure, the chromosome disorganization observed in PICH knockdown cells is not the result of hypotonic treatment during the chromosome spread preparation. Note that the use of nocodazole plus MG132 in the chromosome spread protocol was essential in obtaining consistent chromosome morphologies, because MG132 has been suggested to preserve chromosome structure through regulating cohesin cleavage (Nakajima *et al.*, 2007). We also note that chromosomes that have accumulated GFP-PICH-TA that could no longer target Plk1 to chromosome arms also exhibited a loss of chromosome arm cohesion (Figure 3), as observed in PICH knockdown cells (Figure 4). This result suggests that GFP-PICH-TA alone is not enough to maintain "closed" chromosome arm structure. Together, these data suggest that PICH and cotargeted Plk1 might be important for chromosome arms to maintain chromosome structure.

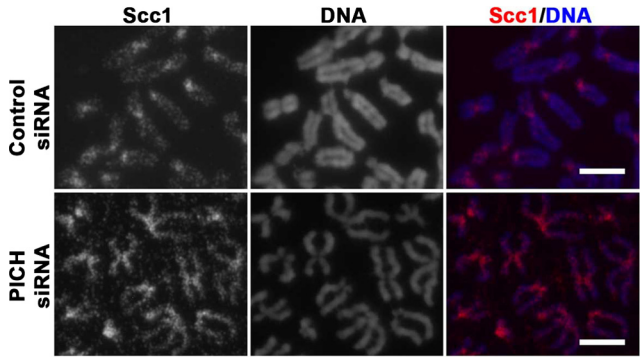

Figure 5. PICH maintains chromosome structure independently of cohesin removal. HeLa cells were treated with siRNA for control or PICH as described in Figure 2B. Chromosome spreads were examined by staining with anti-cohesin subunit Scc1 antibody (red) and counterstained with DAPI (blue). Bars, 10 μm.

Next, because chromosome cohesion seems to be lost in PICH knockdown cells, we examined whether the level of a cohesin subunit Scc1 is reduced on the disorganized chromosomes. During prophase, cohesin is removed in bulk from chromosome arms (Hauf *et al.*, 2005; Gandhi *et al.*, 2006; Kueng *et al.*, 2006), whereas centromere cohesin is removed by separase-mediated cleavage of Scc1 (Uhlmann *et al.*, 2000) during anaphase. In control cells, Scc1 was detected weakly on chromosome arms but strongly at the centromere (Figure 5), as observed by others (Gimenez-Abian *et al.*, 2004). In PICH knockdown cells, in addition to the centromere localization, Scc1 staining was found to spread to the disorganized chromosome arms. Thus, the level of cohesin is not reduced on the disorganized chromosome arms in PICH knockdown cells. These results suggest that the opening of chromosome arms in the highly disorganized chromosomes in PICH-deficient cells is not correlated with the level of cohesin on the chromosome arm.

Chromosome Disorganization in PICH Knockdown Cells Is Prevented by Treatment with Topo II Inhibitor ICRF-193

Because we did not observe a significant change in either the localization or levels of cohesin (Scc1 in Figure 5) or condensin (SMC2 in Figures 2D and 4B) on the disorganized chromosomes arms, we next examined whether interchromatid catenations that intertwine sister chromatids (Diaz-Martinez *et al.*, 2008) might be altered in PICH knockdown cells. Because Topo IIα is required to decatenate DNA to resolve intertwined sister chromatids (Clarke and Lane, 2009), we first examined Topo IIα levels on chromosomes by using anti-Topo IIα antibodies. Immunofluorescence analysis of chromosome spreads showed that Topo IIα levels were equally present in control as well as PICH knockdown cells, and on chromosome arms regardless

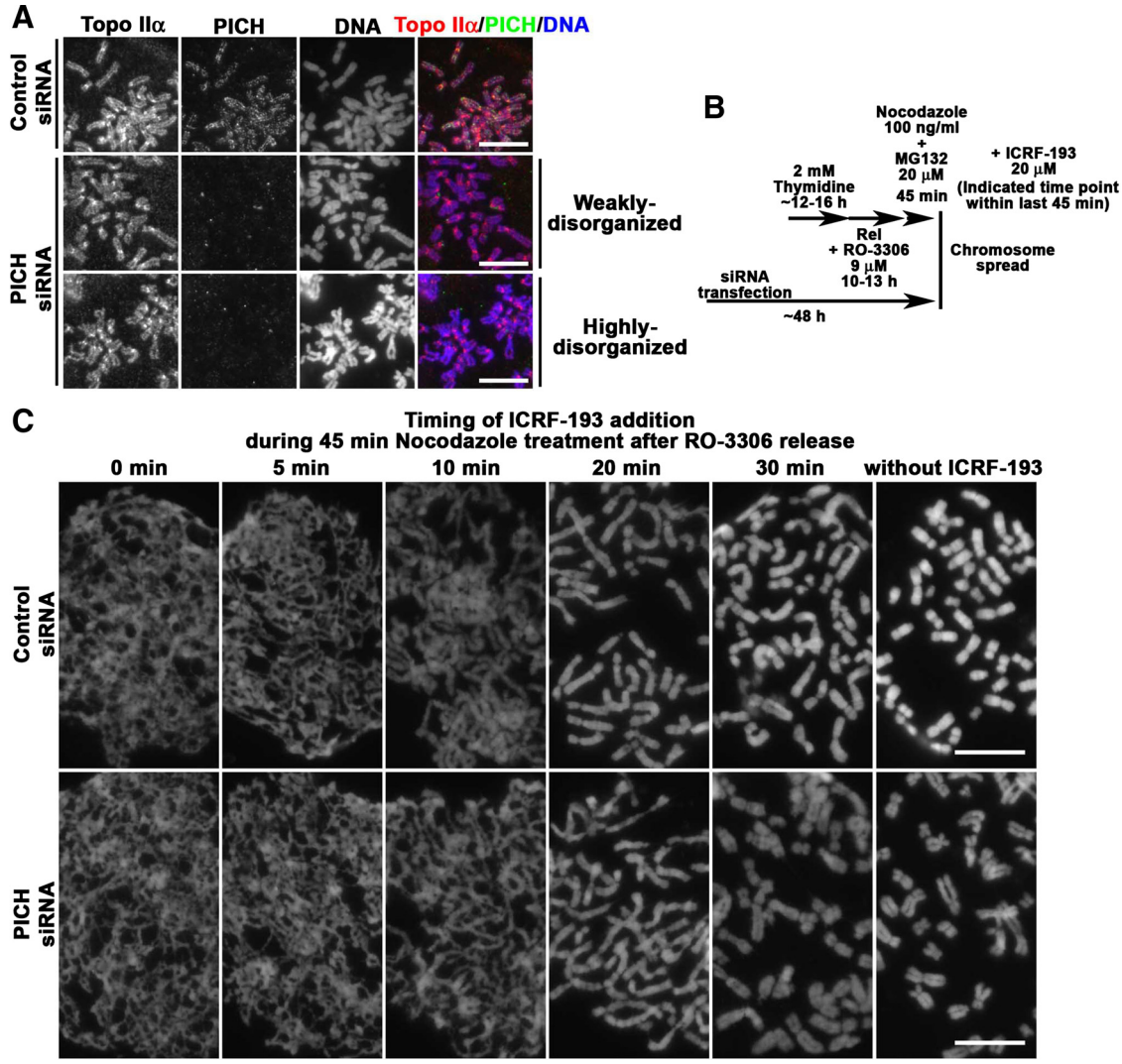

Figure 6. PICH knockdown does not affect Topo II localization on chromosomes or Topo II-dependent chromosome condensation in early prophase. (A) HeLa cells were treated with siRNA for control or PICH for ~48 h. Cells were treated with 2 mM thymidine for 13 h, released into media for 17 h, treated with thymidine again for 22.5 h, released for 5.5 h, and incubated with 50 ng/ml nocodazole plus 20 μM MG132 for 1.5 h. Chromosome spreads were examined by costaining for Topo IIα (red) and PICH (green) and counterstained for DAPI (blue). Both weakly and highly disorganized chromosomes in PICH knockdown cells are shown. Bars, 10 μm. (B and C) HeLa cells were transfected with siRNAs for ~48 h. Cells were treated with 2 mM thymidine for ~12–16 h, released into media containing 9 μM RO-3306 Cdk1 inhibitor for 10–13 h, and released into nocodazole/MG132 for 45 min to examine progression into early prophase (B). ICRF-193 (20 μM) was added to inhibit Topo II activity, either simultaneously with nocodazole/MG132 (0 min) or at 5, 10, 20, or 30 min after the start of nocodazole/MG132 incubation. Cells were incubated for a total of 45 min and harvested. Chromosome spreads were prepared and stained with DAPI for analysis (C). Similar results were obtained in two independent experiments. Bars, 10 μm.

of whether they were weakly or highly disorganized (Figure 6A). These results suggest that PICH knockdown does not affect the localization of Topo IIα on chromosomes.

Next, we used ICRF-193, a Topo II inhibitor (Clarke *et al.*, 1993), to block Topo II activity in PICH knockdown cells. We treated PICH knockdown cells as in Figure 4A, except that the nocodazole/MG132 incubation was for 30 min before 20 μM ICRF-193 was added for another 1.5 h in the continued presence of nocodazole/MG132. Surprisingly, the occurrence of disorganized chromosomes in PICH knockdown cells was dramatically reduced by ICRF-193 treatment, from 85.6% in the absence to 5.9% in the presence of ICRF-193 (Figure 4, B and D, PICH siRNA with/without ICRF-193; $p = 2.57 \times 10^{-4}$). This result suggests that the severe chromosome disorganization observed in PICH knockdown cells could be prevented by treatment with a Topo II inhibitor. Interestingly, although ICRF-193 treatment rescued chromosome structure in PICH knockdown cells, it did not recover Plk1 levels on the chromosome arm (Figures 2E and 4B), suggesting that Plk1 targeting to chromosome arms by PICH lies upstream of the maintenance of chromosome arm architecture. Thus, our data suggest that PICH and cotargeted Plk1 normally maintain chromosome arm architecture and that this process may involve Topo II activity.

Prometaphase Chromosome Architecture, but Not Prophase Chromosome Compaction, Is Regulated by PICH/Plk1

Recently, PICH was suggested to promote chromosome compaction (Leng *et al.*, 2008). However, our data showed

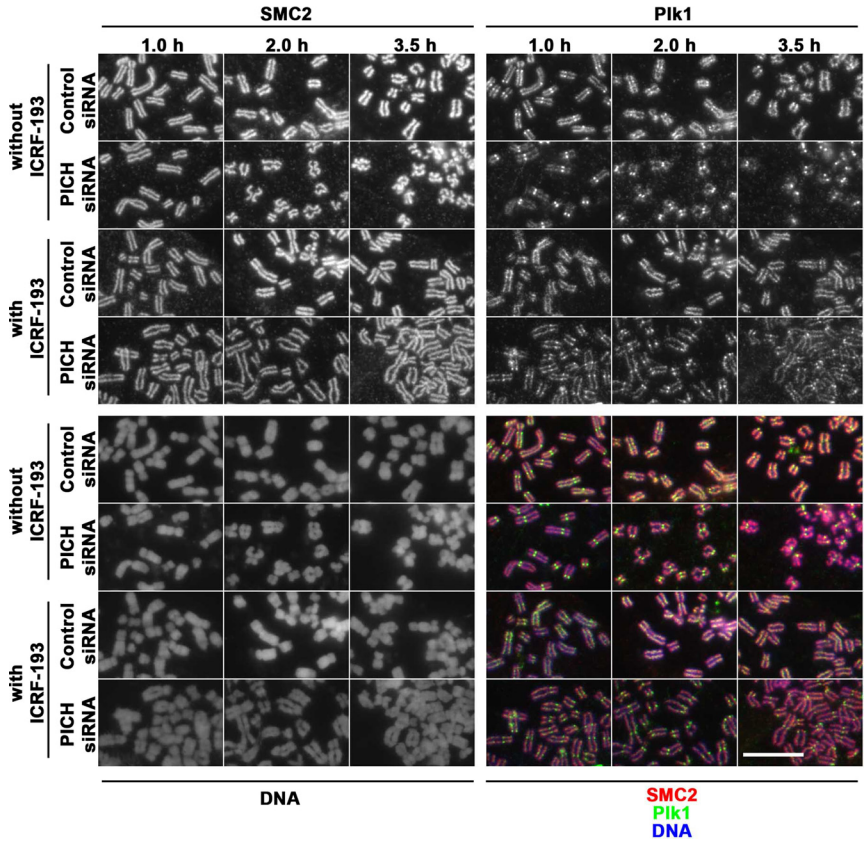

Figure 7. PICH knockdown cells display disorganized chromosome morphology during prometaphase. HeLa cells were treated with siRNA for control or PICH for ~48 h. Cells were synchronized with 2 mM thymidine for ~12–16 h and released into media containing 9 μM RO-3306 for 15 h. Cells were then released into mitosis in the presence of 100 ng/ml nocodazole and 20 μM MG132 for 30 min, further incubated in the presence or absence of 20 μM ICRF-193 for the indicated times, and subjected to chromosome spread preparation. Spreads were stained with anti-SMC2 (red), anti-Plk1 (green) antibodies and counterstained with DAPI (blue). Bar, 10 μm (for all images).

that chromosomes seemed to be more condensed in PICH knockdown cells (Figure 4, B and C), suggesting that PICH may instead inhibit chromosome condensation. To resolve this apparent difference, we examined the role of the PICH–Plk1 complex in chromosome behavior during early mitotic progression. Because ICRF-193 has been shown to block chromosome condensation (Ishida *et al.*, 1991), we used ICRF-193 to examine chromosome condensation during prophase (Figure 6B). PICH knockdown cells were synchronized in the following manner. Cells were treated for ~12–16 h with thymidine, released for 10–13 h into media containing 9 μM RO-3306 and then released in media containing nocodazole plus MG132 for 45 min to allow mitosis progression. During this 45-min incubation with nocodazole and MG132, ICRF-193 was added either simultaneously (0 min after RO-3306 release), progressively later (5, 10, 20, and 30 min after RO-3306 release) or not at all (without ICRF-193) to block chromosome condensation at various times as cells entered early mitosis (Figure 6, B and C). We observed that ICRF-193, when added immediately within the first 10 min of cells entering prophase, blocked the condensation and compaction of chromatin as chromatin remained as thin ribbons rather than highly organized chromosomes (Figure 6C and Supplemental Figure 3). Interestingly, ICRF-193 also blocked chromosome condensation and compaction in PICH knockdown cells in the same time frame (Figure 6C). These results suggest that PICH does not regulate the initial chromosome compaction in prophase.

Next, we examined chromosome morphology of PICH knockdown cells during prometaphase. PICH knockdown cells were synchronized in early mitosis essentially as in Figure 6B, except that cells were enriched in prometaphase by a 30-min incubation with nocodazole plus MG132 before the addition of 20 μM ICRF-193 in the continued presence of nocodazole plus MG132. Chromosome spreads were prepared at different times after ICRF-193 addition, and stained for SMC2 and Plk1 as in Figure 4 to monitor chromosome morphology during prometaphase. With prolonged incubation in nocodazole plus MG132, chromosomes in control cells showed a little more compaction (Figure 7). In contrast, chromosomes in PICH-deficient cells exhibited more wavy and disorganized morphology after 2.0 and 3.5 h in addition to being more compacted. Such a disorganized chromosome phenotype was prevented in the presence of ICRF-193 (Figure 7). These findings are consistent with our interpretation that the initial chromosome compaction during prophase is mediated in part by Topo II in a PICH–Plk1-independent manner (Figure 6C), whereas chromosome architecture during prometaphase is regulated by a PICH/Plk1 complex on the chromosome arms (Figures 4 and 7).

PICH Knockdown Leads to Anaphase DNA Bridge Formation and Failed Abscission

We wondered whether the highly disorganized chromosome structure may impact chromosome segregation and mitotic exit. To investigate this, we examined control versus PICH knockdown cells undergoing unperturbed mitosis using time-lapse live-cell imaging. In PICH-deficient cells, the metaphase plate was less tightly organized than that in control cells (Figure 8A and Supplemental Figure 4), and these less well-organized metaphase plates often led to chromatin bridge formation during anaphase (Figure 8A, arrowheads). These observations raise the possibility that the disorganized chromosomes in prometaphase and metaphase in PICH knockdown cells contributed to chromatin bridges in anaphase. Live-cell imaging analysis clearly showed that

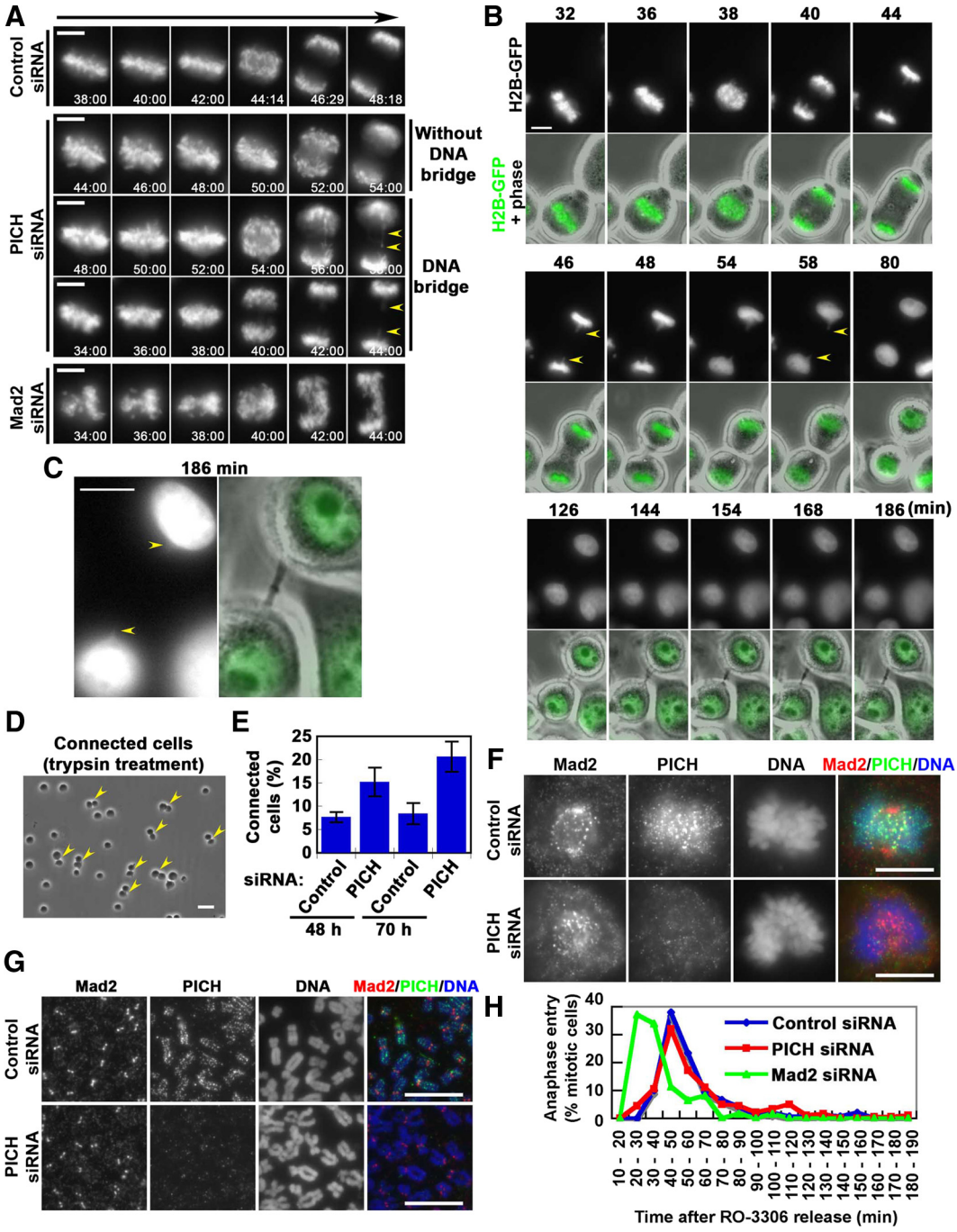

Figure 8. PICH knockdown results in anaphase DNA bridge formation and failed abscission independently of the Mad2-dependent checkpoint mechanism. (A–C) HeLa cells stably expressing H2B-GFP were treated with control, PICH siRNA or Mad2 siRNA oligos for 48 h, synchronized at the G2/M transition with the Cdk1 inhibitor RO-3306, and released into fresh medium (Time = 0). After 10 min of release, live-cell imaging of H2B-GFP fluorescence was initiated, with images captured at 2-min intervals. (See Supplementary Figure 4 for images taken from the beginning.) Representative cells are shown in (A), with arrowheads pointing to DNA bridges. Time-lapse images of a typical PICH knockdown cell (B). Arrowheads point to persistent chromatin bridges from 40 to 186 min after RO-3306 release. Magnified and enhanced (left) images of cells at t = 186 min in B show DNA protrusions (arrowheads) from the connected daughter nuclei (C). (D and E) HeLa cells treated with control or PICH siRNA oligos for 48 h or 70 h were trypsinized and fixed before connected doublet cells (arrowheads in D) were quantified in E. The mean percentage ± SD of connected cells was scored from at least 390 cells in each of three independent experiments (n = 3). (F and G) HeLa cells were treated with control or PICH siRNA oligos for 48 h, stained with anti-Mad2 (red), anti-PICH (green), and counterstained with DAPI (blue), and then they were analyzed in fixed cell (F) or chromosome spread (G) preparations. (H) Live-cell imaging was performed as described in A. Timing of anaphase entry was determined for control, PICH- or Mad2-knockdown cells (n = 150, 181, and 62 cells, respectively) with time 0 set as the time of RO-3306 release. Bars, 10 μm (for all images).

these DNA bridges can persist for an unusually long time (>148 min) (t = 38 to t = 186 min in Figure 8, B and C) and that cells harboring these connections were largely indistinguishable from interphase cells. Thus, to better quantitate

the number of cells that are connected by chromatin bridges, we trypsinized the cells before counting the connected doublet cells (Figure 8D, arrowheads). Using this approach, we found that the number of connected doublet cells increased from 8.4% in controls to 20.7% after PICH knockdown for 3 d (Figure 8E; $p = 1.62 \times 10^{-2}$). This observation suggests that PICH knockdown led to failed abscission due to persistent DNA bridge formation in between the divided cells.

We wondered whether Mad2 mislocalization and perturbed spindle assembly checkpoint initially reported for PICH knockdown cells (Baumann *et al*., 2007) might cause DNA bridge formation and failed abscission. To address this, we examined Mad2 localization in fixed cells and in chromosome spreads. We did not observe any changes in the kinetochore localization of Mad2 after PICH knockdown in either fixed cells (Figure 8F) or chromosome spreads (Figure 8G). Furthermore, we found that PICH-deficient cells progressed through mitosis and entered anaphase with similar kinetics as that in control cells (Figure 8H), in contrast to Mad2-deficient cells that clearly exhibited premature anaphase entry (Figure 8H and Supplemental Figure 4). Together, our data suggest that the anaphase DNA bridges and the resultant failed abscission phenotypes of PICH knockdown are probably a result of chromosome disorganization in prometaphase that is independent of a Mad2-dependent checkpoint mechanism.

DISCUSSION

Sister chromatid resolution is a stepwise process whereby sister chromosomes are resolved from each other during prophase, and complete resolution of sister chromatids is required for chromosomes to separate during anaphase. In this study, we showed that the chromosomal proteins PICH ATPase and Plk1 kinase coordinately maintain sister chromosome architecture during prometaphase and contribute to chromosome resolution. A failure in chromosome resolution in PICH knockdown cells can lead to DNA bridge formation and failed abscission.

Interestingly, prometaphase chromosome disorganization in PICH knockdown cells could be prevented by treatment with a Topo II inhibitor (Figures 4 and 7). This finding raises the intriguing possibility that PICH normally suppresses Topo II decatenating activity in prometaphase and that the absence of PICH can lead to the improper activation of Topo II that results in chromosome disorganization during prometaphase. It is known that the decatenating activity of Topo II in mitosis is crucial for chromosome compaction during early prophase (Ishida *et al*., 1991; Gorbsky, 1994) as well as anaphase chromosome separation (Clarke *et al*., 1993; Gorbsky, 1994). Although the details are not yet clear, we speculate that the PICH–Plk1 complex regulates Topo II activity at these two distinct steps (Figure 9): First, the PICH–Plk1 complex terminates Topo II activity after chromosome compaction; and second, the PICH–Plk1 complex inhibits Topo II function in chromosome decatenation between sister chromatids before their separation (Diaz-Martinez *et al*., 2008; Clarke and Lane, 2009; Nitiss, 2009). This working model can partly explain how chromosome disorganization occurs in PICH knockdown cells (Figure 4). Loss of the PICH–Plk1 complex results in premature activation of Topo II at prometaphase, which leads to prolonged chromosome condensation due to the failure of terminating the early Topo II function. Concurrently, loss of the PICH–Plk1 complex also leads to premature chromosome arm opening due to the inability to inhibit another Topo II function in chromosome separation. The combination of loss of these

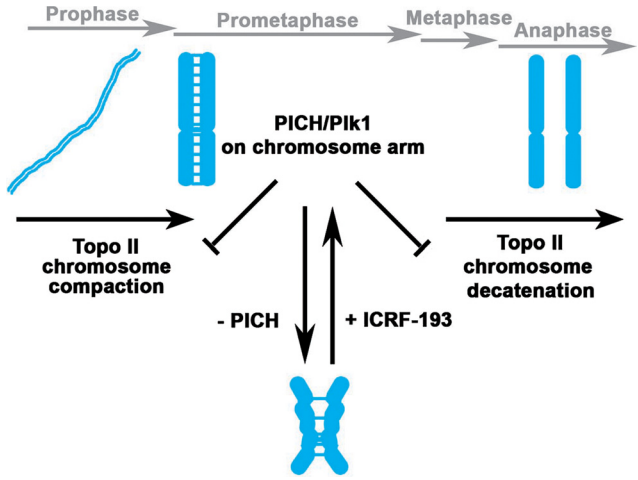

Figure 9. Working model for a PICH/Plk1 complex in maintaining chromosome architecture. See text for details.

two Topo II-dependent functions in PICH knockdown cells would result in the observed highly disorganized chromosomes (Figure 9), that is, more condensed and wavy chromosomes where sister chromatid arms are X-shaped due to the premature loss of arm cohesion. Our findings thus raise the interesting possibility that the temporal inactivation of Topo II at prometaphase by the PICH–Plk1 complex might help Topo II to switch its tasks from chromosome condensation to chromosome separation (Figure 9). The lack of a temporal regulation of Topo II activity in PICH knockdown cells would lead to the accumulation of unresolved DNA links between chromosome arms early in mitosis that would probably cause multiple mitotic defects later, such as persistent DNA bridges and failed abscission (Figure 8). The precise mechanisms involved await further experimentation.

Overexpression of the GFP-PICH-TA mutant (Figure 3) suggests that the Plk1 subpopulation that is targeted to the chromosome arm by PICH contributes to the maintenance of chromosome arm structure. Plk1 may phosphorylate downstream targets on chromosome arms to maintain chromosome arm structure. A recent study showed that Plk1 phosphorylates Topo II in vitro and cells expressing a Plk1 unphosphorylatable mutant Topo II showed chromosome bridge formation in anaphase (Li *et al*., 2008). These findings support our working model in which the PICH–Plk1 complex regulates Topo II activity, albeit to inhibit Topo II activity in prometaphase (Figure 9).

Our working model supports the presence of two Plk1 populations on the chromosome arm, one population that accumulates during prophase and may be involved in the bulk removal of cohesin during prophase (Losada *et al*., 2002; Sumara *et al*., 2002; Gimenez-Abian *et al*., 2004; Hauf *et al*., 2005), and one population that is recruited by PICH to the chromosome arm during prometaphase to maintain chromosome arm architecture (Figure 9). The notion of two populations of Plk1 may explain in part why the morphologies of Plk1-deficient chromosomes by PICH knockdown (disorganized chromosomes with open chromosome arms; Figure 4) versus Plk1-depleted chromosomes by siRNA (rod-shaped and closed chromosome arms; Gimenez-Abian *et al*., 2004; Supplemental Figure 2) are extremely different. The Plk1-depleted chromosomes after Plk1 siRNA have a combined deficiency in both Plk1 subpopulations, where the absence of bulk cohesin removal in prophase (early Plk1 function) may have masked improper chromosome arm

opening in prometaphase (later PICH/Plk1 function in our model), thus sister chromatid arms remain closed. This is consistent with previous suggestions that cohesin removal may be a prerequisite for sister-DNA decatenation (Losada *et al*., 2002). Our study illustrate that differential targeting of Plk1 subpopulations may be essential for mediating sequential events on the chromosome arm.

What regulates the accumulation and/or dissociation of the PICH–Plk1 complex on the chromosome arm? Initially, nuclear membrane breakdown might simply allow the PICH–Plk1 complex access to chromosome arms and thus generate a different Plk1 subpopulation along the chromosome arm. PICH may also be actively recruited to specific sites along chromosome arms (Figure 1B). It is interesting to speculate that the elevated level of PICH on chromosome arms after Plk1 depletion (Baumann *et al*., 2007; Supplemental Figure 2) might be in response to the accumulation of hypercondensed and unresolved catenated chromosomes. As one way to terminate PICH–Plk1 function, phosphoregulation on PICH may be crucial (Baumann *et al*., 2007). Checkpoint silencing may gradually remove Cdk1 phosphorylation on PICH that serves as a docking site for Plk1 (Baumann *et al*., 2007), thereby promoting the dissociation of Plk1 from PICH in anaphase (Figure 1A). In our model, because the PICH–Plk1 complex is primarily responsible for the negative regulation of Topo II activity, the dissociation of Plk1 from chromosomes may be sufficient to allow Topo II reactivation to complete sister chromatid decatenation at the centromere as well as on the chromosome arm.

PICH was originally suggested to be a spindle assembly checkpoint protein that regulates Mad1–Mad2 interaction (Baumann *et al*., 2007). However, a recent study by the same group (Hubner *et al*., 2010) questioned the checkpoint function of PICH. Our data agree with the revised conclusion that PICH does not have a spindle checkpoint function. We did not observe mislocalization of Mad2 from the kinetochore in PICH-depleted cells (Figure 8, F and G), which exhibited normal timing of anaphase entry, in contrast to the premature anaphase onset observed in Mad2 knockdown cells (Figure 8H). Our results show that Mad2-dependent checkpoint is normal in PICH-depleted cells.

Although this study has focused primarily on PICH functions on chromosome arms during prometaphase, PICH is also localized at the centromere (Baumann *et al*., 2007) and may also regulate chromosome resolution at the centromere during anaphase. However, because centromeric catenation at prometaphase was maintained even in the absence of PICH (Figure 4), centromeric DNA decatenation must be inhibited by an additional, probably checkpoint-dependent mechanism (Gimenez-Abian *et al*., 2002). How the PICH–Plk1 complex regulates chromosome decatenation between sister chromatids on either chromosome arms (Funabiki *et al*., 1993; Bhat *et al*., 1996; Sullivan *et al*., 2004; Spence *et al*., 2007; D'Ambrosio *et al*., 2008) and/or centromeres remains to be determined.

ACKNOWLEDGMENTS

We thank M. Nishino for H2B-GFP HeLa cells; S.-H. Lin for assistance with MP-PAb1 antibody generation; J. Qin for assistance with mass spectrometry, GFP-PICH constructs, and the Scc1 antibody; B. R. Brinkley, J. Qin, Y. Wang, M. Leng, M. Nishino, and M. Katoh for helpful discussions; and A. Pigula and J. Pan for technical assistance. This work was supported in part by National Institutes of Health grants DK-53176 and AI071130 (to L.Y.-L.) and grants from the Dan L. Duncan Cancer Center (L.Y.-L.).

REFERENCES

Adachi, Y., Luke, M., and Laemmli, U. K. (1991). Chromosome assembly in vitro: topoisomerase II is required for condensation. Cell *64*, 137–148.

Ahonen, L. J., Kallio, M. J., Daum, J. R., Bolton, M., Manke, I. A., Yaffe, M. B., Stukenberg, P. T., and Gorbsky, G. J. (2005). Polo-like kinase 1 creates the tension-sensing 3F3/2 phosphoepitope and modulates the association of spindle-checkpoint proteins at kinetochores. Curr. Biol. *15*, 1078–1089.

Baumann, C., Korner, R., Hofmann, K., and Nigg, E. A. (2007). PICH, a centromere-associated SNF2 family ATPase, is regulated by Plk1 and required for the spindle checkpoint. Cell *128*, 101–114.

Belmont, A. S. (2006). Mitotic chromosome structure and condensation. Curr. Opin. Cell Biol. *18*, 632–638.

Bhat, M. A., Philp, A. V., Glover, D. M., and Bellen, H. J. (1996). Chromatid segregation at anaphase requires the barren product, a novel chromosome-associated protein that interacts with topoisomerase II. Cell *87*, 1103–1114.

Clarke, D. J., Johnson, R. T., and Downes, C. S. (1993). Topoisomerase II inhibition prevents anaphase chromatid segregation in mammalian cells independently of the generation of DNA strand breaks. J. Cell Sci. *105*, 563–569.

Clarke, D. J., and Lane, A. (2009). Introduction: emerging themes in DNA topoisomerase research. Methods Mol. Biol. *582*, 1–9.

D'Ambrosio, C., Kelly, G., Shirahige, K., and Uhlmann, F. (2008). Condensin-dependent rDNA decatenation introduces a temporal pattern to chromosome segregation. Curr. Biol. *18*, 1084–1089.

Deehan Kenney, R., and Heald, R. (2006). Essential roles for cohesin in kinetochore and spindle function in *Xenopus* egg extracts. J. Cell Sci. *119*, 5057–5066.

Diaz-Martinez, L. A., Gimenez-Abian, J. F., Azuma, Y., Guacci, V., Gimenez-Martin, G., Lanier, L. M., and Clarke, D. J. (2006). PIASgamma is required for faithful chromosome segregation in human cells. PLoS ONE *1*, e53.

Diaz-Martinez, L. A., Gimenez-Abian, J. F., and Clarke, D. J. (2007). Cohesin is dispensable for centromere cohesion in human cells. PLoS ONE *2*, e318.

Diaz-Martinez, L. A., Gimenez-Abian, J. F., and Clarke, D. J. (2008). Chromosome cohesion-rings, knots, orcs and fellowship. J. Cell Sci. *121*, 2107–2114.

Funabiki, H., Hagan, I., Uzawa, S., and Yanagida, M. (1993). Cell cycle-dependent specific positioning and clustering of centromeres and telomeres in fission yeast. J. Cell Biol. *121*, 961–976.

Gandhi, R., Gillespie, P. J., and Hirano, T. (2006). Human Wapl is a cohesin-binding protein that promotes sister-chromatid resolution in mitotic prophase. Curr. Biol. *16*, 2406–2417.

Gimenez-Abian, J. F., Clarke, D. J., Gimenez-Martin, G., Weingartner, M., Gimenez-Abian, M. I., Carballo, J. A., Diaz de la Espina, S. M., Bogre, L., and De la Torre, C. (2002). DNA catenations that link sister chromatids until the onset of anaphase are maintained by a checkpoint mechanism. Eur. J. Cell Biol. *81*, 9–16.

Gimenez-Abian, J. F., Sumara, I., Hirota, T., Hauf, S., Gerlich, D., de la Torre, C., Ellenberg, J., and Peters, J. M. (2004). Regulation of sister chromatid cohesion between chromosome arms. Curr. Biol. *14*, 1187–1193.

Gorbsky, G. J. (1994). Cell cycle progression and chromosome segregation in mammalian cells cultured in the presence of the topoisomerase II inhibitors ICRF-187 [(+)-1,2-bis(3,5-dioxopiperazinyl-1-yl)propane; ADR-529] and ICRF-159 (Razoxane). Cancer Res. *54*, 1042–1048.

Guacci, V., Koshland, D., and Strunnikov, A. (1997). A direct link between sister chromatid cohesion and chromosome condensation revealed through the analysis of MCD1 in *S. cerevisiae*. Cell *91*, 47–57.

Hauf, S., Roitinger, E., Koch, B., Dittrich, C. M., Mechtler, K., and Peters, J. M. (2005). Dissociation of cohesin from chromosome arms and loss of arm cohesion during early mitosis depends on phosphorylation of SA2. PLoS Biol. *3*, e69.

Hirano, T. (2005). Condensins: organizing and segregating the genome. Curr. Biol. *15*, R265–R275.

Hirano, T., and Mitchison, T. J. (1994). A heterodimeric coiled-coil protein required for mitotic chromosome condensation in vitro. Cell *79*, 449–458.

Hubner, N. C., Wang, L. H., Kaulich, M., Descombes, P., Poser, I., and Nigg, E. A. (2010). Re-examination of siRNA specificity questions role of PICH and Tao1 in the spindle checkpoint and identifies Mad2 as a sensitive target for small RNAs. Chromosoma. doi: 10.1007/s00412-009-0244-2.

Ishida, R., Miki, T., Narita, T., Yui, R., Sato, M., Utsumi, K. R., Tanabe, K., and Andoh, T. (1991). Inhibition of intracellular topoisomerase II by antitumor bis(2,6-dioxopiperazine) derivatives: mode of cell growth inhibition distinct from that of cleavable complex-forming type inhibitors. Cancer Res. *51*, 4909–4916.

Kueng, S., Hegemann, B., Peters, B. H., Lipp, J. J., Schleiffer, A., Mechtler, K., and Peters, J. M. (2006). Wapl controls the dynamic association of cohesin with chromatin. Cell *127*, 955–967.

Leng, M., Bessuso, D., Jung, S. Y., Wang, Y., and Qin, J. (2008). Targeting Plk1 to chromosome arms and regulating chromosome compaction by the PICH ATPase. Cell Cycle *7*, 1480–1489.

Li, H., Wang, Y., and Liu, X. (2008). Plk1-dependent phosphorylation regulates functions of DNA topoisomerase IIalpha in cell cycle progression. J. Biol. Chem. *283*, 6209–6221.

Losada, A., Hirano, M., and Hirano, T. (1998). Identification of *Xenopus* SMC protein complexes required for sister chromatid cohesion. Genes Dev. *12*, 1986–1997.

Losada, A., Hirano, M., and Hirano, T. (2002). Cohesin release is required for sister chromatid resolution, but not for condensin-mediated compaction, at the onset of mitosis. Genes Dev. *16*, 3004–3016.

Michaelis, C., Ciosk, R., and Nasmyth, K. (1997). Cohesins: chromosomal proteins that prevent premature separation of sister chromatids. Cell *91*, 35–45.

Nakajima, M., Kumada, K., Hatakeyama, K., Noda, T., Peters, J. M., and Hirota, T. (2007). The complete removal of cohesin from chromosome arms depends on separase. J. Cell Sci. *120*, 4188–4196.

Newport, J., and Spann, T. (1987). Disassembly of the nucleus in mitotic extracts: membrane vesicularization, lamin disassembly, and chromosome condensation are independent processes. Cell *48*, 219–230.

Nitiss, J. L. (2009). DNA topoisomerase II and its growing repertoire of biological functions. Nat. Rev. Cancer *9*, 327–337.

Saka, Y., Sutani, T., Yamashita, Y., Saitoh, S., Takeuchi, M., Nakaseko, Y., and Yanagida, M. (1994). Fission yeast cut3 and cut14, members of a ubiquitous protein family, are required for chromosome condensation and segregation in mitosis. EMBO J. *13*, 4938–4952.

Spence, J. M., Phua, H. H., Mills, W., Carpenter, A. J., Porter, A. C., and Farr, C. J. (2007). Depletion of topoisomerase IIalpha leads to shortening of the metaphase interkinetochore distance and abnormal persistence of PICH-coated anaphase threads. J. Cell Sci. *120*, 3952–3964.

Stegmeier, F., *et al*. (2007). Anaphase initiation is regulated by antagonistic ubiquitination and deubiquitination activities. Nature *446*, 876–881.

Sullivan, M., Higuchi, T., Katis, V. L., and Uhlmann, F. (2004). Cdc14 phosphatase induces rDNA condensation and resolves cohesin-independent cohesion during budding yeast anaphase. Cell *117*, 471–482.

Sumara, I., Vorlaufer, E., Stukenberg, P. T., Kelm, O., Redemann, N., Nigg, E. A., and Peters, J. M. (2002). The dissociation of cohesin from chromosomes in prophase is regulated by Polo-like kinase. Mol. Cell *9*, 515–525.

Toyoda, Y., and Yanagida, M. (2006). Coordinated requirements of human topo II and cohesin for metaphase centromere alignment under Mad2-dependent spindle checkpoint surveillance. Mol. Biol. Cell *17*, 2287–2302.

Uemura, T., Ohkura, H., Adachi, Y., Morino, K., Shiozaki, K., and Yanagida, M. (1987). DNA topoisomerase II is required for condensation and separation of mitotic chromosomes in *S. pombe*. Cell *50*, 917–925.

Uhlmann, F., Wernic, D., Poupart, M. A., Koonin, E. V., and Nasmyth, K. (2000). Cleavage of cohesin by the CD clan protease separin triggers anaphase in yeast. Cell *103*, 375–386.

Vagnarelli, P., Morrison, C., Dodson, H., Sonoda, E., Takeda, S., and Earnshaw, W. C. (2004). Analysis of Scc1-deficient cells defines a key metaphase role of vertebrate cohesin in linking sister kinetochores. EMBO Rep. *5*, 167–171.

Vassilev, L. T., Tovar, C., Chen, S., Knezevic, D., Zhao, X., Sun, H., Heimbrook, D. C., and Chen, L. (2006). Selective small-molecule inhibitor reveals critical mitotic functions of human CDK1. Proc. Natl. Acad. Sci. USA *103*, 10660–10665.

Wang, L. H., Schwarzbraun, T., Speicher, M. R., and Nigg, E. A. (2008). Persistence of DNA threads in human anaphase cells suggests late completion of sister chromatid decatenation. Chromosoma *117*, 123–135.

Wood, E. R., and Earnshaw, W. C. (1990). Mitotic chromatin condensation in vitro using somatic cell extracts and nuclei with variable levels of endogenous topoisomerase II. J. Cell Biol. *111*, 2839–2850.

Xu, Y. X., and Manley, J. L. (2007). New insights into mitotic chromosome condensation: a role for the prolyl isomerase Pin1. Cell Cycle *6*, 2896–2901.